Inorganic Chemistry
Communication

Inorg. Chem. **2010**, *49*, 5335–5337 **5335**
DOI: 10.1021/ic9025427

Triphenylamine-Modified Ruthenium(II) Terpyridine Complexes: Enhancement of Light Absorption by Conjugated Bridging Motifs

Kiyoshi C. D. Robson, Bryan D. Koivisto, Terry J. Gordon, Thomas Baumgartner, and Curtis P. Berlinguette*

Department of Chemistry and Institute for Sustainable Energy, Environment & Economy, University of Calgary, 2500 University Drive NW, Calgary, Alberta, Canada T2N-1N4

Received December 20, 2009

The photophysical properties of a family of heteroleptic $[Ru(tpy)_2]^{2+}$ (tpy = 2,2′:6′,2″-terpyridine) complexes modified with triphenylamine donor units with different bridging units are reported.

The design of molecules for light-harvesting applications requires structural elements that balance a myriad of electronic properties.[1] Compounds with high molar extinction coefficients (ε) often feature a highest occupied molecular orbital (HOMO) distributed over a significant portion of the molecule and a spatially separated lowest unoccupied molecular orbital (LUMO). Organic chromophores designed for dye-sensitized solar cells,[2] for example, often contain a conjugated linker between the donor (D) and acceptor (A) groups, an arrangement that facilitates a light-driven $\pi-\pi^*$ transition.[3,4] Ruthenium(II) polypyridyl complexes, on the other hand, typically make use of a metal-to-ligand charge-transfer (MLCT) process for use in light-harvesting applications.[5] While ε values are usually lower for ruthenium-based dyes relative to their organic counterparts, the absorption profiles of the metal complexes are generally broader and are extended to longer wavelengths, thereby offering greater utility in solar energy conversion schemes.[6]

Taking these collective observations into account, we set out to combine the favorable attributes of organic and inorganic chromophores in pursuit of molecules with intense, low-energy electronic transitions. To realize these hybridized systems, we installed the triphenylamine (TPA) donor motif common to organic dyes[3,7,8] onto a ligand platform capable of binding to a metal [i.e., 2,2′:6′,2″-terpyridine (tpy)]. There is limited precedent for polypyridyl ruthenium complexes containing terminal TPA substituents,[9−11] and even fewer examples exist where conjugated linkers are installed between the coordinating ligand fragment and the TPA group.[12,13] In this work, we incorporate acetylene and 2,5-thiophene linkers, which serve to circumvent steric repulsion between adjacent aromatic six-membered rings, between the {Ru(tpy)} and TPA units of **1** (Figure 1). An evaluation of the photophysical properties

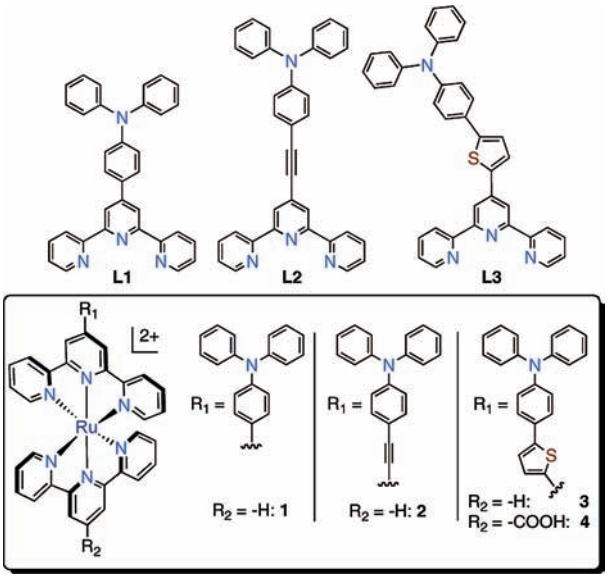

Figure 1. Structural representations of ligands **L1**−**L3** and complexes **1**−**4** (counterion = NO_3^-) investigated in this study.

*To whom correspondence should be addressed. E-mail: cberling@ucalgary.ca.

(1) Campagna, S.; Puntoriero, F.; Nastasi, F.; Bergamini, G.; Balzani, V. *Top. Curr. Chem.* **2007**, *280*, 117–214.
(2) O'Regan, B.; Grätzel, M. *Nature* **1991**, *353*, 737–740.
(3) Hagberg, D. P.; Marinado, T.; Karlsson, K. M.; Nonomura, K.; Qin, P.; Boschloo, G.; Brinck, T.; Hagfeldt, A.; Sun, L. *J. Org. Chem.* **2007**, *72*, 9550–9556.
(4) Mishra, A.; Fischer, M. K. R.; Bauerle, P. *Angew. Chem., Int. Ed.* **2009**, *48*, 2474–2499.
(5) Ardo, S.; Meyer, G. J. *Chem. Soc. Rev.* **2009**, *38*, 115–164.
(6) Grätzel, M. *Inorg. Chem.* **2005**, *44*, 6841–6851.
(7) Hagberg, D. P.; Edvinsson, T.; Marinado, T.; Boschloo, G.; Hägfeldt, A.; Sun, L. C. *Chem. Commun.* **2006**, 2245–2247.
(8) Ning, Z.; Tian, H. *Chem. Commun.* **2009**, 5483–5495.
(9) Bonhote, P.; Moser, J.-E.; Humphry-Baker, R.; Vlachopoulos, N.; Zakeeruddin, S. M.; Walder, L.; Grätzel, M. *J. Am. Chem. Soc.* **1999**, *121*, 1324–1336.
(10) Collin, J. P.; Guillerez, S.; Sauvage, J. P.; Barigelletti, F.; De Cola, L.; Flamigni, L.; Balzani, V. *Inorg. Chem.* **1991**, *30*, 4230–8.
(11) Handa, S.; Wietasch, H.; Thelakkat, M.; Durrant, J. R.; Haque, S. A. *Chem. Commun.* **2007**, 1725–1727.
(12) Karthikeyan, C. S.; Peter, K.; Wietasch, H.; Thelakkat, M. *Sol. Energy Mater. Sol. Cells* **2007**, *91*, 432–439.
(13) Karthikeyan, C. S.; Wietasch, H.; Thelakkat, M. *Adv. Mater.* **2007**, *19*, 1091–1095.

Published on Web 05/18/2010

Table 1. Electronic Absorption and Emission Data for **L1**−**L3** and **1**−**5**

	UV−vis data[a]		emission data[c]		
	λ_{max}[b] (nm)	ε (M^{-1} cm^{-1})	λ_{em} (nm) (λ_{ex} (nm))	τ (ns) (χ^2)	Φ[d]
L1	361	29 300	498 (400)	6.6 (1.05)	0.15
L2	376	27 200	530 (400)	4.9 (0.83)	0.23
L3	395	25 100	542 (400)	3.7 (0.81)	0.29
1	493	29 300	660 (493)	1.1 (0.86)	1.8×10^{-4}[f]
	414	12 300	[e]		
2	498	34 900	689 (509)	18 (1.11)	9.6×10^{-4}[f]
	430 (sh)	17 900	538 (425)	4.6 (1.10)	
3	505	42 000	720 (510)	410 (0.98)	< 0.01
	440 (sh)	19 400	549 (425)	3.4 (1.18)	
4	508	44 200	723 (510)	580 (0.97)	< 0.03
	445 (sh)	20 200	548 (425)	3.5 (1.16)	
5	475	15 500	619 (449)		

[a] Collected in CH_3OH. [b] Values corresponding to lowest-energy maxima, and shoulders (sh) are reported. [c] Collected in CH_3CN. [d] Absolute values; measured with an integrating sphere unless noted otherwise. [e] Not observed. [f] Relative to $[Ru(bpy)_3]^{2+}$ in MeCN: 0.059.[14]

that arise from the varying degrees of electronic coupling between these neighboring chromophore units is detailed herein.

The syntheses of TPA-substituted tpy ligands **L1**−**L3** were all achieved in reasonably high yields on a relatively large scale (Scheme S1 in the Supporting Information). Coordination of **L1**−**L3** to the synthon $[Ru(tpy\text{-}R_2)Cl_3]$ (R_2 = −H, −COOH) yields hybridized organic/inorganic chromophores **1**−**4**. The structural identities of all ligands and complexes were confirmed by a combination of NMR spectroscopy, mass spectrometry, and/or elemental analysis (see the Supporting Information).

The cyclic voltammograms for **L1**−**L3** and **1**−**4** all reveal a reversible oxidation wave ($E_{1/2}^{ox}$) ascribed to oxidation of the TPA unit (i.e., TPA/$TPA^{\bullet+}$). The proximity of the electron-withdrawing pyridine and alkyne groups of **L1** and **L2** increases the oxidation potential by 150 and 160 mV, respectively, relative to the thiophene spacer of **L3** ($E_{1/2}^{ox}$ = 1.38, 1.39, and 1.23 V vs NHE for **L1**−**L3**, respectively). In the absence of a conjugated linker, the electron-withdrawing character of the tpy fragment is significantly diminished upon ligation to the metal, thereby rendering the TPA unit more susceptible to oxidation ($E_{1/2}^{ox}$ for **1** is observed at 1.26 V vs NHE). Conversely, the inclusion of either a thiophene or alkyne spacer results in a TPA oxidation potential that is effectively unaltered upon ligation; i.e., the $E_{1/2}^{ox}$ values of 1.38, 1.24, and 1.24 V vs NHE for **2**−**4**, respectively, are congruent with the formal oxidation potentials of the corresponding free ligands. Scanning to higher potentials reveals an irreversible signal that is assigned to the oxidation of the $TPA^{\bullet+}$ unit; a reversible Ru^{II}/Ru^{III} redox couple could not be delineated. The ligands are not reduced within the solvent window, but the corresponding metal complexes show two *pseudo*reversible reduction waves at ca. −0.8 and −1.2 V vs NHE (Table S1 in the Supporting Information), which are assigned to successive reductions of the tpy ligand and the opposing TPA-tpy fragment.

Electronic absorption and emission data for **L1**−**L3**, **1**−**4**, and benchmark complex $[Ru(tpy)_2](PF_6)_2$ (**5**) in MeOH are provided in Table 1. The absorption bands centered in the 350−450 nm range for **L1**−**L3** are ascribed to intraligand charge-transfer (ILCT) transitions (Figure S1 in the Supporting Information). While ligand **L1** is subject to steric interactions between protons of adjacent six-membered rings, insertion of the acetylene and thiophene spacers circumvents these interactions, resulting in a bathochromic shift of the absorption band maxima (λ_{max}) for **L2** and **L3**. The longer λ_{max} value for **L2** relative to **L1** is ascribed to the electron-withdrawing character of the alkyne linker, lowering the LUMO. Similarly, the low-resonance energy of the thiophene unit stabilizes the LUMO.

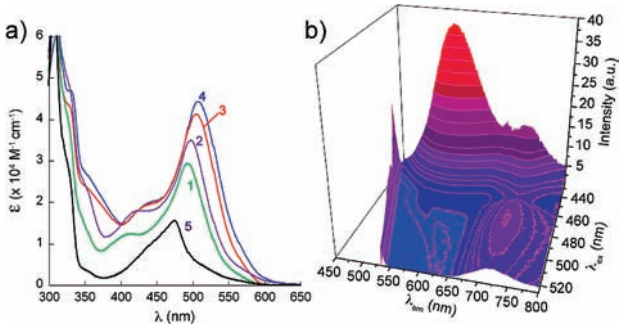

Figure 2. (a) Absorption profiles for **1**−**5** in CH_3OH (counterion = NO_3^- for **1**−**4**; PF_6^- for **5**). (b) Three-dimensional emission profiles for **4** in MeCN as a function of the excitation wavelength (λ_{ex}).

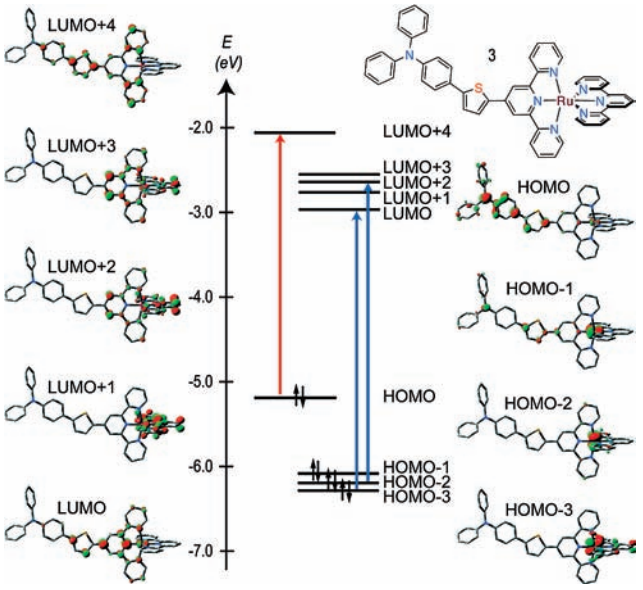

Figure 3. Principle electronic transitions for **3** predicted by TD-DFT. The ILCT (red) and MLCT (blue) transitions are offset for clarity (Ru = magenta; N = blue; S = gold).

The absorption profiles for **1**−**4** over the 375−600 nm range each contain a broad, intense band centered at ca. 500 nm with a higher-energy shoulder (or peak) between 400 and 450 nm (Figure 2a). Both features display a sensitivity to the identity of the spacer in terms of the intensity and position of the absorbance bands. The maxima of the lowest-energy absorption bands are bathochromically shifted by 132, 122, and 110 nm and progressively more intense for **1**−**3**, respectively, relative to the free ligand (Table 1). The ε value for **1** is 2-fold greater than that of **5**, which highlights the positive effect that the D−A arrangement of the TPA-tpy motif has on the absorption profiles of ruthenium(II) coordination complexes of this type. The higher ε values (and longer λ_{max} values) for **2**−**4** relative to **1** are manifest in the enhanced conjugation between the D and A units.

Time-dependent density functional theory (TD-DFT) indicates that the ILCT transitions for **L1**−**L3** are maintained when ligated to the metal center in **1**−**3**, respectively. The principle electronic transitions predicted for **3** in solution (MeCN) are presented in Figure 3. These results indicate that an ILCT process originating from the TPA unit (HOMO → LUMO+4) makes a significant contribution to the lower-energy absorbance band, while the shoulder centered at ca. 440 nm consists of transitions that are predominantly MLCT in character (e.g., HOMO−2 → LUMO+2 and HOMO−3 → LUMO). Similar observations were made for **1**, **2**, and **4**, but symmetry considerations predict fewer transitions for **1** and **2** (Figure S2 in the Supporting Information). The significant intensity of the absorbance band for **1**−**3** is attributed to the confluence of these ILCT and MLCT transitions. Spectroelectrochemical experiments confirm that a combination of ILCT and MLCT transitions comprises both bands, with the lower-energy band being primarily ILCT in character (Figure S3 in the Supporting Information).

Emission measurements reveal similar Stokes shifts (ca. 150 nm), excited-state lifetimes (3−7 ns), and quantum yields (0.15−0.29) for **L1**−**L3** (Table 1). Tracking the wavelength-dependent emission behavior of the metal complexes reveals dual-emission behavior for **2**−**4** (Figure 2b), an uncommon feature among ruthenium(II) complexes.[15−17] The dominant ILCT character within the low-energy absorption bands for **1**−**4** is corroborated by monitoring the emission at variable excitation wavelengths (Figures 2b and S4 in the Supporting Information). Excitation of **3** (or **4**) at 425 nm generates two emission bands at ca. 550 and 725 nm, while irradiation at longer wavelengths (e.g., 510 nm) only generates the lower-energy emission band. Complex **1** does not exhibit dual-emission behavior, which is in accordance with related compounds that lack spacers between the donor substituent and the tpy ligand.[10] Note that **1** is also the only complex in this study that exhibits electronic communication between the TPA and Ru center in the ground state on the basis of electrochemistry experiments. Dual emission is observed for **2**, but the excited-state lifetime of the lower-energy emission band is significantly lower than that of **3** and **4**. We contend that this discrepancy is due to the lower rotational barrier of the alkyne spacer, providing access to nonradiative decay pathways. The dual-emission behavior is assigned to decay from a single excited state to the spatially separated TPA and Ru chromophores (Scheme 1). Transient absorption spectroscopy studies are underway to unambiguously elucidate these processes.

Scheme 1. Qualitative Description of Key Radiative and Nonradiative Processes for **2**−**4**[a]

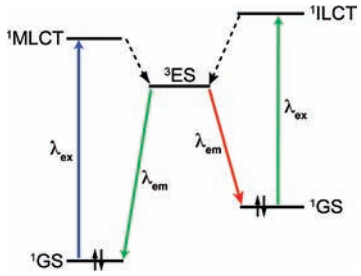

[a] Radiative and nonradiative decay processes indicated by solid and dashed arrows, respectively; GS = ground state; ES = emissive state.

This work demonstrates the profound effect that the TPA group, with a judicious choice of the conjugated spacer, has on the photophysical properties of $[Ru(tpy)_2]^{2+}$ complexes. Of the complexes used in this investigation, the influence of the D−A arrangement on the optical properties is most pronounced in the case where the thiophene is used as the bridging unit (i.e., **3** and **4**). This observation is ascribed to the polarizability and low resonance energy of the thiophene spacer, promoting a planar arrangement between the TPA and tpy units. This notion is validated by TD-DFT calculations and by the relative excited-state lifetimes for the metal complexes. The observed lifetimes can also be rationalized by the spatial proximity of the excited-state electron density to the TPA unit. This trend is also consistent with enhanced intersystem crossing mediated by the Ru^{II} center.[14]

Ligand systems with the TPA moiety attached to polypyridyl ligands are not without precedent but have not been exhaustively developed to date.[9,11−13] This examination serves to elaborate on these studies by evincing the role that the spacer unit has on the photophysical properties of these types of complexes. The principle objective of this study was realized in establishing that large increases in the ε values (and excited-state lifetimes) are observed when appropriate conjugated spacer units are positioned between the TPA donor group and the {Ru(tpy)} acceptor fragment. Studies are currently underway to explore the utility of these complexes in artificial photosynthetic frameworks.

Acknowledgment. This work was financially supported by the Canadian Natural Science and Engineering Research Council, Canada Research Chairs, Canadian Foundation for Innovation, Alberta Innovates, and the Canada School of Energy and Environment. K.C.D.R. is grateful for an NSERC graduate scholarship.

Supporting Information Available: Synthetic details and TD-DFT, (spectro)electrochemical, and optical data. This material is available free of charge via the Internet at http://pubs.acs.org.

(14) Juris, A.; Balzani, V.; Barigelletti, F.; Campagna, S.; Belser, P.; Von Zelewsky, A. *Coord. Chem. Rev.* **1988**, *84*, 85–277.
(15) Tyson, D. S.; Luman, C. R.; Zhou, X.; Castellano, F. N. *Inorg. Chem.* **2001**, *40*, 4063–4071.
(16) Blakley, R. L.; Myrick, M. L.; DeArmond, M. K. *J. Am. Chem. Soc.* **1986**, *108*, 7843–7844.
(17) Wang, X.-Y.; Del Guerzo, A.; Tunuguntla, H.; Schmehl, R. H. *Res. Chem. Intermed.* **2007**, *33*, 63–77.